

Temporal hierarchy and context-dependence of quorum sensing signal in *Pseudomonas aeruginosa*

Stoyko Katarov¹ & Volker Behrends^{1,*}

¹ The Centre for Integrated Research in Life and Health Sciences, University of Roehampton; volker.behrends@roehampton.ac.uk

* Correspondence: volker.behrends@roehampton.ac.uk

Simple Summary: The bacterium *Pseudomonas aeruginosa* is one of the main pathogens that patients can contract in hospitals. We were interested in how nutrients around a bacterium shape its behavior. We looked at the molecules that bacteria use to communicate and how what they eat influences whether they grow as free-swimming cells or multicellular aggregates attached to surfaces. We found that one of the main regulators of both behavior and virulence is significantly impacted by media composition, highlighting that the cell's environment needs to be understood and could be exploited to improve treatment.

Abstract: The Gram-negative bacterium *Pseudomonas aeruginosa* can cause infections in a broad range of hosts including plants, invertebrate and mammals and is an important source of nosocomial infections in humans. We were interested in how differences in the bacteria's nutritional environment impact bacterial communication and virulence factor production. We grew *P. aeruginosa* in 96 different conditions in BIOLOG Gen III plates and assayed quorum sensing (QS) signaling over the course of growth. We also quantified pyocyanin and biofilm production and the impact of sub-inhibitory exposure to Tobramycin. We found that while 3-oxo-C12 homoserine lactone remained the dominant QS signal to be produced, timing of PQS production differed between media types. Further, whether cells grew predominantly as biofilms or planktonic cells was highly context dependent. Our data suggest that understanding the impact of the nutritional environment on the bacterium can lead to valuable insights into the link between bacterial physiology and pathology.

Keywords: mass spectrometry; ESKAPE pathogens; *Pseudomonas aeruginosa*; quorum sensing; hierarchy; sub-MIC antibiotics

Citation: Katarov, S.; Behrends, V.; Temporal hierarchy and context-dependence of quorum sensing signal in *Pseudomonas aeruginosa*. *Life* **2022**, *12*, x. <https://doi.org/10.3390/xxxxx>

Academic Editor: Firstname Last-name

Received: date

Accepted: date

Published: date

Publisher's Note: MDPI stays neutral with regard to jurisdictional claims in published maps and institutional affiliations.



Copyright: © 2022 by the authors. Submitted for possible open access publication under the terms and conditions of the Creative Commons Attribution (CC BY) license (<https://creativecommons.org/licenses/by/4.0/>).

1. Introduction

Pseudomonas aeruginosa is an important opportunistic pathogen that has been shown to cause infections in plants, invertebrates, and vertebrates[1]. In humans, the pathogen can cause eye, ear, or toe infections in healthy, immunocompetent people. Importantly, in healthcare settings, *P. aeruginosa* is responsible for burn wound and catheter-associated urinary tract infections as well as ventilator- and general healthcare-associated pneumonia [2,3]. Further, *P. aeruginosa* has been associated with long, chronic infections of the airways of people with cystic fibrosis (CF)[4–7].

Part of its pathogenic success is due to *P. aeruginosa*'s metabolic flexibility [6,8], its high resistance to antibiotics [9] and its large array of virulence factors [6,10–12]. These factors include different types of protein secretion systems and secreted proteins [13]. Depending on the type of secretion system, proteins are either secreted into the cell's environment or directly injected into the target cell. The complement of effector proteins, more specifically whether the cell carries ExoU (a phospholipase) or ExoS (a bi-functional toxin with GTPase-activating protein and adenosine diphosphate ribosyl transferase activity),

determines whether strains of *P. aeruginosa* are invasive or cytotoxic [14–16]. Other virulence factors include siderophores (pyoverdine, pyochelin[17]), redox-active phenazines and their derivative pyocyanin [18] as well as the toxin cyanide [19].

The regulation of several of these virulence factors occurs via quorum sensing (QS)[20,21], particularly if the cells are in a planktonic state [6,12,21]. *P. aeruginosa* has three interconnected QS systems (the *lasR*, *rhlR* and the *pqs* systems), but several environmental and physiological cues are integrated into these systems [22]. The signaling molecules of the *las* and *rhl* systems are acyl-homoserine lactones (HSLs), namely 3-oxo-dodecanoyl-HSL (3oC12-HSL) and butyryl-HSL (C4-HSL), respectively. The *pqs* (or Pseudomonas quinolone signal) molecule is 2-heptyl-3-hydroxy-4-quinolone, but other, structurally related alkyl quinolone (AQ) compounds with specific biological functions exist [23,24]. QS controls up to 10% of gene expression of *P. aeruginosa*[25]. In planktonic cells, several virulence factors, e.g., elastase, pyocyanin, and cyanide are QS-controlled. Conversely, the Type-3-secretion system is repressed by QS [26].

Several studies have investigated context-dependence of biofilm formation [27] and eradication [28], virulence factor production [8,18,29,30] and/or antimicrobial resistance [31–34], though usually in a limited number of conditions at one time-point. Here, we were interested to investigate the interaction of cell number/growth phase and growth environment on different QS systems to elucidate their impact on virulence factor and biofilm production. We performed intermittent sampling across the growth curves in 96 conditions in a BIOLOG GenIII plate and quantified QS signal, the virulence factor pyocyanin (by mass spectrometry) as well biofilm production after 24h. We found that while QS hierarchy follows expected patterns in rich media, the expression of virulence factors and biofilm formation was highly context dependent.

2. Materials and Methods

Pseudomonas aeruginosa wild-type PA14, a strain original isolated due to its ability to infect plants as well as vertebrates [1], was grown in Luria Bertani (LB) broth (10 g/L NaCl, 10 g/L tryptone and 5g/l yeast extract) overnight at 37°C, shaking at 150 rpm. From these, starter cultures were inoculated by 1:100 dilution and left to grow until they reached an optical density at 600nm of 0.6. At that point, 2ml of the culture was harvested by centrifugation (5min, 3,000xg, RT), the supernatant discarded and the pellet washed and resuspended in 1 ml 10 mM phosphate buffered saline, pH 7. The process was repeated and the resuspended cells were mixed with 10 ml inoculation fluid A and inoculated into BIOLOG Gen III plates (both BIOLOG, Hayward, CA, USA).

At 3, 5.5, 8, 11, 14, 17 and 20 hours, readings at OD₅₉₅ (for metabolic activity/oxidative metabolism) and OD₇₅₀ (cell number) were taken and 25 µl of culture were sampled, centrifuged (2,000xg, 2min, RT) and stored at -20°C for extraction of QS molecules. After 24h, we also assayed surface-attached biofilm formation using the crystal violet method [35]. To assess the impact of sub-inhibitory exposure to Tobramycin, treated plates were mixed with 0.8 µg/ml Tobramycin at inoculation and sampled after 20h only.

To extract QS compounds, 10 µl of the supernatants were mixed with 90 µl acetonitrile (LC-MS grade) containing 0.1% formic acid (w/v), 1uM heptyl homoserine lactone and 4-cyclohexyl-2(1H)-quinolone (for normalization of HSLs and PQS, respectively; both Merck, Darmstadt, Germany) and frozen at -20°C for 1h. For analysis, 10 µl of each sample were transferred to a high-recovery plate and mixed with 90 µl LC-MS grade water (Fisher Scientific).

Detection of QS compounds by tandem mass spectrometry was based on a method published by Ortori et al. [36]. Separation was achieved on a Waters Acquity H Class Ultra Performance Liquid Chromatography (UPLC) system using a Waters HSS T3 UPLC column (2.1 mm X 100 mm, 1.8 µm particle size, equipped with a HSS T3 VanGuard pre-column) maintained at 45°C. The UPLC system used 0.1% formic acid (in water) with 0.1 mM EDTA as phase A and 0.1% formic acid (in acetonitrile) as phase B. The gradient

was 1% B for 0.75 min, then up to 35% B at 1.5 min, 75% B at 3 min and 99% B at 3.75 min. At 4.25 min, the system switched back to 1% B, which was held for 0.75 min.

Mass Spectra were obtained on a Waters TQSmicro triple quad mass spectrometer with electrospray ionization in positive mode using multiple reaction monitoring. The source potential was 3.5kV with the source held at 450°C and a desolvation gas flow of 650 L/hr. Transitions and mass spectral parameters (cone and collision voltages) were originally taken from [36] and optimized by manual infusion of 10 µM standard (at 10µl/min) for C4-HSL, 3-oxo-C12-HSL, pyocyanin, PQS and HHQ. Biological quality control samples were injected every eight samples to control for drift in instrument sensitivity. Data analysis, including baseline correction and QC batch correction was carried out in Matlab using in-house scripts (modified from [37]).

3. Results

3.1. General growth characteristics on BIOLOG Gen III

BIOLOG Gen III plates contain 71 single carbon sources, one negative control (no carbon source), 23 sensitivity test conditions (rich media with a 'stressor') and one positive control (rich media only). While the single carbon source assay the ability of *P. aeruginosa* to grow on a substrate, the sensitivity test condition investigate the ability of the bacterium to overcome the 'stressor' (e.g. high salt stress or an antibiotic) in rich medium. To check which of these conditions supported oxidative metabolism (tetrazolium dye reduction) or measurable cell replication, we monitored optical densities at two wavelengths, 595 nm and 750 nm, respectively. Naturally, different condition produced a high variety of outcomes with regards to growth rate and optical density reached after 20h (Fig. 1). Using exclusion criteria of reaching 10% of the recorded overall maximum value over the course of growth, we concluded that 52 conditions supported metabolic activity, 43 supported growth and 42 supported both, respectively (Fig. 1, Tab. A1).

Surface-attached biofilm was detectable in several conditions of the BIOLOG Gen III plate after 24h of growth (Fig. 2). There is no clear correlation between measured optical cell density (highest value at 750 nm) and biofilm development, but there is some grouping based on media type. Cultures grown on single carbon sources supported lower planktonic cell numbers than the sensitivity assays, which have a rich base medium (Fig. 2A/B, Tab. S1). The median ratio of biofilm formation to planktonic growth was significantly higher in single carbon sources than in sensitivity assays (median 2.26 vs 0.86 for maximum-normalised optical density values, respectively, $p < 0.001$, Student's t-test).

The temporal hierarchy of bacterial communication systems showed some variation between conditions (Fig. 3A/B). In most wells, including the positive control (well A10), which contains a rich medium not unlike LB media routinely used for studies of pseudomonas QS, 3oC12-HSL was clearly produced before C4-HSL and PQS, in line with the established hierarchy of QS systems in *P. aeruginosa* [20]. 3oC12-HSL was produced at fairly low cell densities and declined as peak cell numbers were reached, while C4-HSL and PQS levels increased more or less in line with cell number (median R2 to cell number (Pearson) 0.13, 0.86 and 0.83 for 3oC12-HSL, C4-HSL and PQS, respectively (Fig. 1/3)).

Interestingly, there is a clear difference with regards to stationary phase PQS levels. They increased with cell number in many conditions, but, in sensitivity assays, PQS levels rose with cell number and stayed near their maximum or even continued to increase for the recorded growth period. In most single carbon sources, PQS levels

increase before cell number, peaked around 11h post-inoculation and declined after that (Fig. 3B). When investigating per-cell virulence factor production (pyocyanin per cell number) in the different condition sets, there are clear condition-dependent differences (Fig. 3C). The per-cell pyocyanin production is about 20-30 fold higher in acetic acid-grown cultures or rich media supplemented with D-serine than in cultures grown at pH 5, respectively. When total levels of pyocyanin and PQS produced over the course of growth are compared and plotted against metabolic activity, it is evident that while overall correlation is good ($R^2 = 0.76$ and 0.90 , for pyocyanin and PQS respectively), context-specific differences exist. For pyocyanin, production is generally lower than expected based on metabolic activity in a range of sensitivity assays (Fig. 3D). For PQS, levels are higher than expected in wells with a sugar or disaccharide as the single carbon source (Fig. 3D).

Finally, we were interested in the context-dependent impact of sub-inhibitory antibiotic exposure (Tab. 1). Metabolic activity did not exhibit a clear general trend (median \log_2 fold change across conditions of 0.02), but did exhibit a range of over six \log_2 units (log₂ median fold change (log mfc) 3.99 for Bromosuccinate to -2.16 for Formic acid). Cellular growth and 3oC12-HSL exhibited similar profiles with median log mfc of 0.34 and 0.28 , respectively and ranges of log mfc from 3.76 (Gluconic acid) to -1 (Potassium Tellurite) for cellular growth and log mfc from 4.33 (Citric Acid) to -1.98 (Propionic Acid) for 3oC12-HSL, respectively.

However, for the two other QS systems as well as pyocyanin there was a clear negative impact of Tobramycin exposure. The impact was moderate for C4-HSL and PQS. The median across conditions was of -1.26 and -1.36 with ranges from -2.81 (Propionic Acid) to -0.07 (Malic acid) and from -3.39 (Potassium Tellurite) to -0.13 (Gelatin), respectively. In contrast, the impact on pyocyanin production was pronounced, with a median across conditions of -3.12 \log_2 units and ranges of log mfc from a value of -9.17 (Propionic Acid) to log mfc -1.1 (pH 5).

3.2. Figures, Tables and Schemes

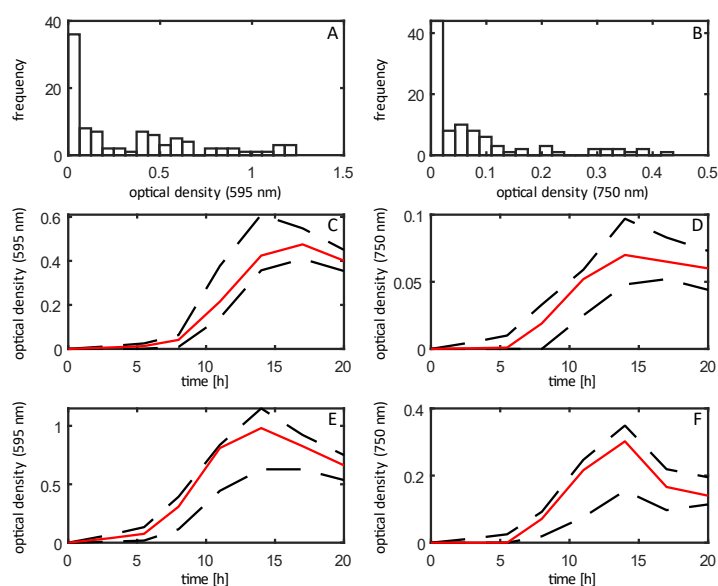


Figure 1. Optical density across growth conditions on a BIOLOG GenIII plate. (A) Histogram of absorbance values recorded at 595 nm, (B) histogram of absorbance values recorded at 750 nm, (C) median (red line) and interquartile range (dashed black lines) of absorbance recorded at 595 nm for substrates supporting growth in wells A1-H9 (single carbon sources), (D) median (red line) and interquartile range (dashed black lines) of absorbance recorded at 750 nm for substrates supporting growth in wells A1-H9 (single carbon sources), (E) median (red line) and interquartile range (dashed black lines) of absorbance recorded at 595 nm for substrates supporting growth in wells I1-H9 (disaccharide sources), (F) median (red line) and interquartile range (dashed black lines) of absorbance recorded at 750 nm for substrates supporting growth in wells I1-H9 (disaccharide sources).

interquartile range (dashed black lines) of absorbance recorded at 750 nm for substrates supporting growth in wells A1-H9 (single carbon sources), (E) median (red line) and interquartile range (dashed black lines) of absorbance recorded at 595 nm for substrates supporting growth in wells A10-H12 (sensitivity assays), (F) median (red line) and interquartile range (dashed black lines) of absorbance recorded at 750 nm for substrates supporting growth in wells A10-H12 (single carbon sources).

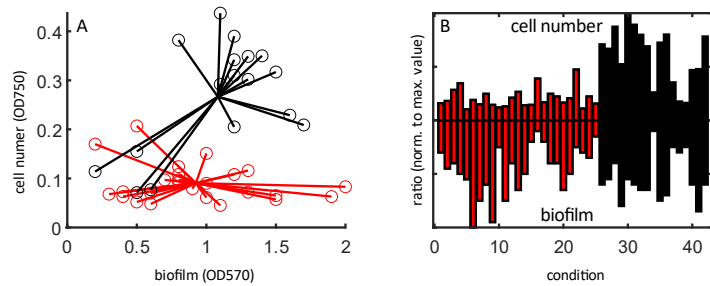
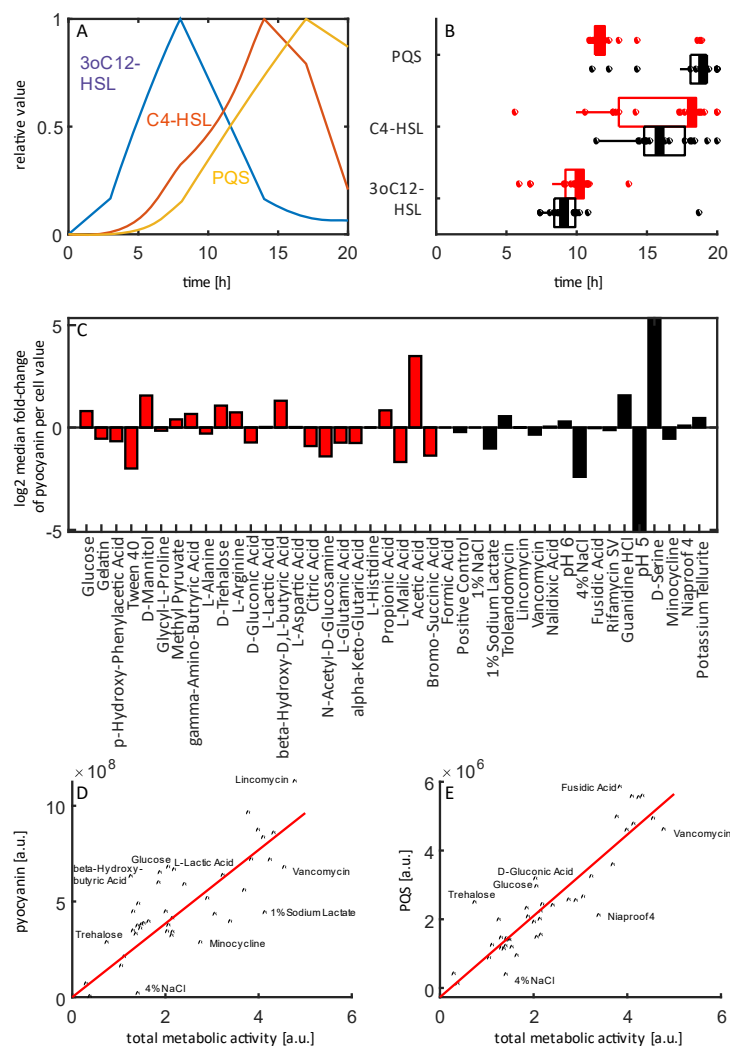


Figure 2. Context-dependent relationship between surface-attached biofilm and planktonic cell growth across conditions in the BIOLOG Gen III plate. (A) Scatter graph of growth-supporting condition, red: single carbon sources, black: sensitivity assays. (B) Bar chart displaying the ratio of planktonic and biofilm growth. Values were normalized to highest value across growth-supporting conditions, colors as (A).



177
178
179
180
181

182

183
184
185
186
187
188

189

Figure 3. Temporal and cell-density dependence of QS and virulence factor production. (A) Temporal hierarchy of QS system in rich media (positive control, well A10), normalized to highest value, (B) Representation of temporal hierarchy of the three major QS systems across all growth-supporting conditions. Red: Single carbon sources, black: Sensitivity assays. Box and whisker plots represent median, interquartile range and extent of data range. (C) Median fold change of pyocyanin-cell number ratio. Single carbon sources and Sensitivity assays were divided to their own median. Red: Single carbon sources, black: Sensitivity assays. (D) Scatter plot of total metabolic activity and pyocyanin produced over the course of growth, (E) Scatter plot of total metabolic activity and PQS produced over the course of growth.

Table 1. Impact of sub-inhibitory exposure to Tobramycin (0.8µg/ml) on metabolic activity, cellular growth the three QS systems and pyocyanin production. Values are expressed as log₂ fold change of the treated vs. the control samples.

		activity	cell number	3oC12-HSL	C4-HSL	PQS	pyocyanin
Glucose	C1	0.08	0.01	0.50	-0.73	-0.58	-2.69
Gelatin	E1	2.17	0.72	0.10	-0.55	-0.13	-1.67
p-Hydroxy-Phenylacetic Acid	G1	-1.27	1.08	-0.42	-1.43	-1.36	-3.74
Tween 40	H1	-0.78	0.03	0.61	-0.73	-0.83	-4.11
D-Mannitol	D2	0.13	-0.02	-1.01	-2.03	-1.83	-2.36
Glycyl-L-Proline	E2	0.33	1.53	0.14	-1.29	-0.79	-2.25
Methyl Pyruvate	G2	0.15	0.00	-0.14	-1.00	-0.63	-1.61
gamma-Amino-Butyric Acid	H2	-0.84	-0.27	0.42	-0.88	-1.22	-2.33
L-Alanine	E3	-0.08	0.82	1.62	-0.79	-1.26	-2.58
D-Trehalose	A4	-0.14	-0.02	-0.74	-1.74	-1.80	-2.97
L-Arginine	E4	0.13	1.88	0.88	-1.82	-1.97	-4.88
D-Gluconic Acid	F4	0.06	3.76	0.30	-1.55	-0.88	-3.27
L-Lactic Acid	G4	0.26	1.71	1.54	-1.01	-0.60	-3.44
beta-Hydroxy-D,L-butyric Acid	H4	-0.71	0.70	0.86	-1.31	-1.46	-4.17
L-Aspartic Acid	E5	0.26	1.60	0.17	-0.81	-1.46	-2.16
Citric Acid	G5	-0.13	-0.32	4.33	-0.60	-1.29	-3.31
N-Acetyl-D-Glucosamine	B6	0.38	-0.03	0.56	-1.41	-1.00	-3.36
L-Glutamic Acid	E6	0.19	0.16	0.42	-2.14	-1.66	-4.23
alpha-Keto-Glutaric Acid	G6	-0.02	2.87	0.71	-1.73	-1.68	-4.03
L-Histidine	E7	0.34	1.12	-0.28	-1.67	-1.37	-2.75
Propionic Acid	H7	0.00	0.00	-1.98	-2.81	-2.27	-9.17
L-Malic Acid	G8	0.12	0.24	0.28	-0.07	-1.51	-4.70
Acetic Acid	H8	0.00	0.00	2.90	-1.42	-2.55	-7.23
Bromo-Succinic Acid	G9	3.99	0.00	0.21	-0.22	-0.38	-1.33
Formic Acid	H9	-2.16	0.00	-0.63	-1.44	-0.65	-4.73
Positive Control	A10	-0.19	0.18	0.34	-1.23	-1.71	-4.12
1% NaCl	B10	-0.17	0.15	-0.15	-0.13	-1.35	-2.17
1% Sodium Lactate	C10	0.13	0.43	0.66	-0.77	-1.27	-3.52

Troleandomycin	D10	0.42	1.64	-1.75	-1.40	-1.05	-1.81
Lincomycin	E10	0.00	0.00	0.55	-0.85	-1.30	-1.90
Vancomycin	F10	-0.04	0.04	0.29	-1.02	-1.48	-2.79
Nalidixic Acid	G10	0.15	0.56	0.50	-0.74	-1.36	-2.11
pH 6	A11	0.24	1.49	-0.56	-1.50	-1.53	-2.70
4% NaCl	B11	0.57	1.48	-0.28	-0.10	-0.56	-1.21
Fusidic Acid	C11	-0.10	0.44	-0.21	-1.71	-2.18	-4.03
Rifamycin SV	D11	0.03	0.58	-0.81	-1.92	-2.31	-3.92
Guanidine HCl	E11	0.32	2.58	-0.59	-0.90	-1.18	-2.27
pH 5	A12	-0.78	1.89	-0.88	-0.72	-0.88	-1.10
D-Serine	C12	-0.62	0.00	1.07	-0.51	-1.55	-2.67
Minocycline	D12	-0.20	0.48	1.38	-2.10	-1.75	-4.11
Niaproof 4	E12	-0.29	-0.11	-0.22	-1.29	-1.58	-3.88
Potassium Tellurite	G12	-0.41	-1.00	2.82	-1.66	-3.39	-5.51

202

203

4. Discussion

204

We compared growth and quorum sensing signaling dynamics, virulence factor (pyocyanin) production and impact of sub-inhibitory antibiotic exposure across 96 different growth conditions in BIOLOG GenIII plates. We found several differences, but also similarities across growth-supporting conditions.

205

206

207

208

For most growth-supporting conditions, *P. aeruginosa* maintained the top-level QS hierarchy with 3oC12-HSL the first signal to be produced. The prominent exception was cells grown at pH 5, but this is likely connected to the very slow growth in the condition. A second similarity was that planktonic growth mostly depended on media type, not individual carbon source. Rich media-based sensitivity tests (wells A10-H12) in general supported growth to higher optical densities than single carbon sources within the timeframe of the experiment. In contrast, surface-attached biofilm production over the first 24h of growth did not correlate to media type.

209

210

211

212

213

214

215

216

Interestingly, there is a large variance in planktonic/biofilm partitioning in the different carbon source/conditions. The lowest relative levels of biofilm were found in cells grown in citric acid and rich media supplemented with 1% sodium lactate. This is in line with previous findings in the literature. *P. aeruginosa* cultures grown on citric acid have been shown to have altered biofilm morphology in a flow-cell model [38] and decreased biofilm production in a process dependent on the TctD-TctE two component system [39]. Sodium lactate led to decrease in biofilm production in *Shewanella putrefaciens* [40]. The process is dependent on LrbS-LrbA-LrbR, which is thought to have similar functions to RocS1, RocR and RocA1 in *P. aeruginosa* [41]. In *Pseudomonas*, RocS1A1R regulate the expression of Cup adhesion proteins, essential for biofilm formation [42].

217

218

219

220

221

222

223

224

225

226

The highest relative levels of biofilm were found in cultures grown on arginine and alanine, respectively. This agrees with previous literature, as arginine was found to be crucial for the formation of biofilms in bacterial-epithelial cell interaction models [43]. There are also mechanistic links that tie arginine to high biofilm production. It can be used as a nitrate donor [44] and high NO₃ is linked to elevated biofilm production [45],

227

228

229

230

231

while its denitrification product NO leads to biofilm dispersal [28]. Interestingly, the *rhl* QS system, which represses the transcription of denitrification genes [46] is partially regulated by arginine availability due to a rare arginine codon on the *rhlR* mRNA [47]. We did not see a change in biofilm levels (relative to the positive control) if the media was supplemented with D-Serine. D-amino acids have been suggested to lead to biofilm dispersal, though this has been disputed recently [48,49].

Temporal hierarchy for C4-HSL and PQS also differed due to media type, though with considerable spread. In minimal media, PQS levels peaked earlier than in rich media/sensitivity assays and decayed towards the end of the observed growth period. One explanation is the iron chelation ability of PQS [50]. The compound could be upregulated in minimal media and enzymatically degraded to increase iron availability in stationary phase [51]. An important caveat to consider is that we are effectively measuring a planktonic-biofilm hybrid and that the crystal violet-based method ignores floating cell aggregates, which might differ in their physiology from both planktonic cells and surface-attached biofilms [52]. Further, it has been suggested recently that during surface attachment, the regulatory cascade with 3oC12-HSL promoting C4-HSL and PQS production does not fully apply [53–57]. Rather, the production of cytotoxic alkyl quinolones seems to be driven by a process involving type IV pili and the surface sensor PilY1 [56,58,59]. Finally, in established biofilms (the formation of which is also controlled by QS [20,21]), virulence is generally thought to be lower than in planktonic or surface-attaching states [9,60].

PQS has been suggested previously to have a multifaceted role in *P. aeruginosa*, acting – among others – as QS signal [23,24], an iron chelator [50], a live/death signal via oxidative stress in *Pseudomonas* itself [61], an initiator of oxidative stress in host cells [62], a photosensitizer [63] and/or a warning signal of antibiotic stress on population level [64]. In our setting, we compared oxidative metabolic activity to PQS levels and found that – while generally well correlated – higher than expected levels of PQS in cultures grown on sugars and lower than expected levels of PQS in some sensitivity conditions. Given the multitude of roles, changes in PQS are likely to be seen due to different triggers and should be investigated further.

Finally, we found that sub-inhibitory exposure to 1/10x MIC Tobramycin had marked impact on C4-HSL, PQS and pyocyanin production. Generally, virulence factor production is thought to be downregulated upon sub-inhibitory antibiotic exposure, often through down-regulation of QS, though variety exists among studies [6,12]. Carbon sources were differentially impacted by antibiotic exposure, further confirming the impact of nutritional context on antibiotic tolerance [32,33,65].

5. Conclusions

Overall, our study highlights the context-dependence of bacterial QS, mode of growth and resistance. Understanding the specifics of these interactions can lead to improvements in bacterial treatment. Therefore, nutritional environments of infection sites should be surveyed and recreated in the laboratory to make models of infection more realistic. Future work should expand on this study using additional strains, e.g. clinical isolates from CF patients to take into account the evolutionary history in different niches.

Supplementary Materials: The following supporting information can be downloaded at: www.mdpi.com/xxx/s1, Table S1: An overview of the conditions of the BIOLOG Gen III plate.

Author Contributions: Conceptualization, V.B.; methodology, V.B.; software, V.B.; data acquisition, S.K., V.B.; writing—original draft preparation, S.K., V.B.; writing—review and editing, V.B.; All authors have read and agreed to the published version of the manuscript.

Funding: This research was funded by the Society for Applied Microbiology Students to Work grant. 281
282

Institutional Review Board Statement: Not applicable. 283

Informed Consent Statement: Not applicable. 284

Conflicts of Interest: The authors declare no conflict of interest. 285
286

Appendix A 287

Table A1: An overview of the conditions of the BIOLOG Gen III plate and whether the met the criteria for supporting metabolic activity and/or cellular growth. 288
289

Name	Well	Metabolic activity	Planktonic growth	Both	Biofilm	ratio bf/cell
Negative Control	A1					
D-Raffinose	B1					
Glucose	C1	x	x	x	x	1.87
D-Sorbitol	D1					
Gelatin	E1	x	x	x	x	2.49
Pectin	F1				x	
p-Hydroxy-Phenylacetic Acid	G1	x	x	x	x	1.41
Tween 40	H1	x	x	x	x	1.45
Dextrin	A2					
Lactose	B2				x	
D-Mannose	C2				x	
D-Mannitol	D2	x	x	x	x	5.34
Glycyl-L-Proline	E2	x	x	x	x	5.27
D-Galacturonic Acid	F2	x				
Methyl Pyruvate	G2	x	x	x	x	5.04
gamma-Amino-Butyric Acid	H2	x	x	x	x	2.43
D-Maltose	A3					
D-Melibiose	B3					
D-Fructose	C3	x			x	
D-Arabitol	D3	x			x	
L-Alanine	E3	x	x	x	x	6.59
L-Galactonic Acid Lactone	F3					
D-Lactic Acid Methyl Ester	G3					
alpha-Hydroxy-Butyric Acid	H3				x	
D-Trehalose	A4	x	x	x	x	2.10
alpha-Methyl-D-Glucoside	B4					
D-Galactose	C4					
myo-Inositol	D4					
L-Arginine	E4	x	x	x	x	5.75
D-Gluconic Acid	F4	x	x	x	x	1.90
L-Lactic Acid	G4	x	x	x	x	2.45

beta-Hydroxy-D,L-butyric Acid	H4	x	x	x	x	3.58
D-Cellobiose	A5					
D-Salicin	B5					
3-Methyl Glucose	C5					
Glycerol	D5	x			x	
L-Aspartic Acid	E5	x	x	x	x	1.39
D-Glucuronic Acid	F5	x				
Citric Acid	G5	x	x	x	x	0.26
alpha-Keto-Butyric Acid	H5				x	
Gentiobiose	A6					
N-Acetyl-D-Glucosamine	B6	x	x	x	x	1.20
D-Fucose	C6	x				
D-Glucose-6-PO4	D6					
L-Glutamic Acid	E6	x	x	x	x	1.62
Glucuronamide	F6	x				
alpha-Keto-Glutaric Acid	G6	x	x	x	x	1.80
Acetoacetic Acid	H6					
Sucrose	A7					
N-Acetyl-D-Mannosamine	B7					
L-Fucose	C7					
D-Fructose-6-PO4	D7	x			x	
L-Histidine	E7	x	x	x	x	3.95
Mucic Acid	F7					
D-Malic Acid	G7				x	
Propionic Acid	H7	x	x	x	x	2.43
D-Turanose	A8					
N-Acetyl-D-Galactosamine	B8					
L-Rhamnose	C8					
D-Aspartic Acid	D8					
L-Pyroglutamic Acid	E8	x			x	
Quinic Acid	F8				x	
L-Malic Acid	G8	x	x	x	x	0.53
Acetic Acid	H8	x	x	x	x	2.73
Stachyose	A9					
N-Acetyl Neuraminic Acid	B9					
Inosine	C9	x			x	
D-Serine_single	D9					
L-Serine	E9				x	
D-Saccharic Acid	F9					
Bromo-Succinic Acid	G9	x	x	x	x	1.58
Formic Acid	H9	x	x	x	x	0.96

Positive Control	A10	x	x	x	x	0.85
1% NaCl	B10	x	x	x	x	0.82
1% Sodium Lactate	C10	x	x	x	x	0.46
Troleandomycin	D10	x	x	x	x	1.53
Lincomycin	E10	x	x	x	x	0.55
Vancomycin	F10	x	x	x	x	0.67
Nalidixic Acid	G10	x	x	x	x	0.81
Aztreonam	H10					
pH 6	A11	x	x	x	x	0.94
4% NaCl	B11	x	x	x	x	0.38
Fusidic Acid	C11	x	x	x	x	1.03
Rifamycin SV	D11	x	x	x	x	0.87
Guanidine HCl	E11	x	x	x	x	0.70
Tetrazolium Violet	F11					
Lithium Chloride	G11					
Sodium Butyrate	H11				x	
pH 5	A12	x	x	x	x	1.70
8% NaCl	B12		x			
D-Serine	C12	x	x	x	x	1.54
Minocycline	D12	x	x	x	x	1.28
Niaproof 4	E12	x	x	x	x	1.78
Tetrazolium Blue	F12					
Potassium Tellurite	G12	x	x	x	x	0.77
Sodium Bromate	H12					
Total		52	43	42	57	

290

References

291

1. Rahme, L.G.; Stevens, E.J.; Wolfort, S.F.; Shao, J.; Tompkins, R.G.; Ausubel, F.M. Common Virulence Factors for Bacterial Pathogenicity in Plants and Animals. *Science* **1995**, *268*, 1899–1902, doi:10.1126/science.7604262. 292
2. Turner, K.H.; Everett, J.; Trivedi, U.; Rumbaugh, K.P.; Whiteley, M. Requirements for *Pseudomonas Aeruginosa* Acute Burn and Chronic Surgical Wound Infection. *PLoS Genet* **2014**, *10*, e1004518, doi:10.1371/journal.pgen.1004518. 293
3. Reynolds, D.; Kollef, M. The Epidemiology and Pathogenesis and Treatment of *Pseudomonas Aeruginosa* Infections: An Update. **2021**, *81*, 2117–2131, doi:10.1007/s40265-021-01635-6. 294
4. Folkesson, A.; Jelsbak, L.; Yang, L.; Johansen, H.K.; Ciofu, O.; Høiby, N.; Molin, S. Adaptation of *Pseudomonas Aeruginosa* to the Cystic Fibrosis Airway: An Evolutionary Perspective. *Nat Rev Microbiol* **2012**, *10*, 841–851, doi:10.1038/nrmicro2907. 295
5. Williams, H.D.; Davies, J.C. Basic Science for the Chest Physician: *Pseudomonas Aeruginosa* and the Cystic Fibrosis Airway. *Thorax* **2012**, *67*, 465–467, doi:10.1136/thoraxjnl-2011-201498. 296
6. Dolan, S.K. Current Knowledge and Future Directions in Developing Strategies to Combat *Pseudomonas Aeruginosa* Infection. *J Mol Biol* **2020**, *432*, 5509–5528, doi:10.1016/j.jmb.2020.07.021. 297

302

303

304

305

306

7. Nolan, C.; Behrends, V. Sub-Inhibitory Antibiotic Exposure and Virulence in *Pseudomonas Aeruginosa*. *Antibiotics (Basel)* **2021**, *10*, doi:10.3390/antibiotics10111393. 307
308
8. Behrends, V.; Bell, T.J.T.J.; Liebeke, M.; Cordes-Blauert, A.; Ashraf, S.N.S.N.S.N.; Nair, C.; Zlosnik, J.E.A.J.E.A.; Williams, H.D.H.D.; Bundy, J.G.J.G.J.G.J.G. Metabolite Profiling to Characterize Disease-Related Bacteria: Gluconate Excretion by *Pseudomonas Aeruginosa* Mutants and Clinical Isolates from Cystic Fibrosis Patients. *J Biol Chem* **2013**, *288*, 15098–15109, doi:10.1074/jbc.M112.442814. 309
310
311
312
9. Moradali, M.F.; Ghods, S.; Rehm, B.H.A. *Pseudomonas Aeruginosa* Lifestyle: A Paradigm for Adaptation, Survival, and Persistence. *Front Cell Infect Microbiol* **2017**, *7*, 39, doi:10.3389/fcimb.2017.00039. 313
314
10. Hauser, A.R. *Pseudomonas Aeruginosa*: So Many Virulence Factors, so Little Time. *Crit Care Med* **2011**, *39*, 2193–2194, doi:10.1097/CCM.0b013e318221742d. 315
316
11. Jurado-Martín, I.; Sainz-Mejías, M.; Mcclean, S. Molecular Sciences *Pseudomonas Aeruginosa*: An Audacious Pathogen with an Adaptable Arsenal of Virulence Factors. **2021**, doi:10.3390/ijms22063128. 317
318
12. Nolan, C.; Behrends, V.; Imperi, F. Antibiotics Sub-Inhibitory Antibiotic Exposure and Virulence in *Pseudomonas Aeruginosa*. **2021**, doi:10.3390/antibiotics10111393. 319
320
13. Filloux, A. Protein Secretion Systems in *Pseudomonas Aeruginosa*: An Essay on Diversity, Evolution, and Function. *Front Microbiol* **2011**, *2*, 155, doi:10.3389/fmicb.2011.00155. 321
322
14. Sana, T.G.; Berni, B.; Bleves, S. The T6SSs of *Pseudomonas Aeruginosa* Strain PAO1 and Their Effectors: Beyond Bacterial-Cell Targeting. *Front Cell Infect Microbiol* **2016**, *6*, 61, doi:10.3389/fcimb.2016.00061. 323
324
15. Sana, T.G.; Baumann, C.; Merdes, A.; Soscia, C.; Rattei, T.; Hachani, A.; Jones, C.; Bennett, K.L.; Filloux, A.; Superti-Furga, G.; et al. Internalization of *Pseudomonas Aeruginosa* Strain PAO1 into Epithelial Cells Is Promoted by Interaction of a T6SS Effector with the Microtubule Network. *mBio* **2015**, *6*, e00712, doi:10.1128/mBio.00712-15. 325
326
327
328
16. Jolly, A.L.; Takawira, D.; Oke, O.O.; Whiteside, S.A.; Chang, S.W.; Wen, E.R.; Quach, K.; Evans, D.J.; Fleiszig, S.M.J. *Pseudomonas Aeruginosa*-Induced Bleb-Niche Formation in Epithelial Cells Is Independent of Actinomyosin Contraction and Enhanced by Loss of Cystic Fibrosis Transmembrane-Conductance Regulator Osmoregulatory Function. *mBio* **2015**, *6*, e02533, doi:10.1128/mBio.02533-14. 329
330
331
332
17. Lee, K.; Lee, K.-M.; Go, J.; Ryu, J.-C.; Ryu, J.-H.; Yoon, S.S. The Ferrichrome Receptor A as a New Target for *Pseudomonas Aeruginosa* Virulence Attenuation. *FEMS Microbiol Lett* **2016**, *363*, doi:10.1093/femsle/fnw104. 333
334
335
18. Jo, J.; Price-Whelan, A.; Cornell, W.C.; Dietrich, L.E.P. Interdependency of Respiratory Metabolism and Phenazine-Associated Physiology in *Pseudomonas Aeruginosa* PA14. *J Bacteriol* **2020**, *202*, doi:10.1128/JB.00700-19. 336
337
338
19. Williams, H.D.; Zlosnik, J.E.A.; Ryall, B. *Oxygen, Cyanide and Energy Generation in the Cystic Fibrosis Pathogen Pseudomonas Aeruginosa*; 2006; Vol. 52; ISBN 0120277522. 339
340
20. Williams, P.; Winzer, K.; Chan, W.C.; Cámara, M. Look Who's Talking: Communication and Quorum Sensing in the Bacterial World. *Philos Trans R Soc Lond B Biol Sci* **2007**, *362*, 1119–1134, doi:10.1098/rstb.2007.2039. 341
342
343
21. Lee, J.; Zhang, L. The Hierarchy Quorum Sensing Network in *Pseudomonas Aeruginosa*. *Protein Cell* **2015**, *6*, 26, doi:10.1007/S13238-014-0100-X. 344
345
22. Williams, P.; Cámara, M. Quorum Sensing and Environmental Adaptation in *Pseudomonas Aeruginosa*: A Tale of Regulatory Networks and Multifunctional Signal Molecules. *Curr Opin Microbiol* **2009**, *12*, 182–191, doi:10.1016/j.mib.2009.01.005. 346
347
348

23. Dubern, J.-F.; Diggle, S.P. Quorum Sensing by 2-Alkyl-4-Quinolones in *Pseudomonas Aeruginosa* and Other Bacterial Species. *Mol Biosyst* **2008**, *4*, 882–888, doi:10.1039/b803796p. 349
350
24. Heeb, S.; Fletcher, M.P.; Chhabra, S.R.; Diggle, S.P.; Williams, P.; Cámara, M. Quinolones: From Antibiotics to Autoinducers. *FEMS Microbiol Rev* **2011**, *35*, 247–274, doi:10.1111/j.1574-6976.2010.00247.x. 351
352
25. Schuster, M.; Greenberg, E.P. A Network of Networks: Quorum-Sensing Gene Regulation in *Pseudomonas Aeruginosa*. *Int J Med Microbiol* **2006**, *296*, 73–81, doi:10.1016/j.ijmm.2006.01.036. 353
354
26. Pena, R.T.; Blasco, L.; Ambroa, A.; González-Pedrajo, B.; Fernández-García, L.; López, M.; Bleriot, I.; Bou, G.; García-Contreras, R.; Wood, T.K.; et al. Relationship Between Quorum Sensing and Secretion Systems. *Front Microbiol* **2019**, *10*, 1100, doi:10.3389/fmicb.2019.01100. 355
356
357
27. Haney, E.; Trimble, M.; Cheng, J.; Vallé, Q.; Hancock, R. Critical Assessment of Methods to Quantify Biofilm Growth and Evaluate Antibiofilm Activity of Host Defence Peptides. *Biomolecules* **2018**, *8*, 29, doi:10.3390/biom8020029. 358
359
360
28. Sauer, K.; Cullen, M.C.; Rickard, A.H.; Zeef, L.A.H.; Davies, D.G.; Gilbert, P. Characterization of Nutrient-Induced Dispersion in *Pseudomonas Aeruginosa* PAO1 Biofilm. *J Bacteriol* **2004**, *186*, 7312–7326, doi:10.1128/JB.186.21.7312-7326.2004. 361
362
363
29. Linares, J.F.; Moreno, R.; Fajardo, A.; Martínez-Solano, L.; Escalante, R.; Rojo, F.; Martínez, J.L. The Global Regulator Crc Modulates Metabolism, Susceptibility to Antibiotics and Virulence in *Pseudomonas Aeruginosa*. *Environ Microbiol* **2010**, *12*, 3196–3212, doi:10.1111/j.1462-2920.2010.02292.x. 364
365
366
30. Huang, J.; Sonnleitner, E.; Ren, B.; Xu, Y.; Haas, D. Catabolite Repression Control of Pyocyanin Biosynthesis at an Intersection of Primary and Secondary Metabolism in *Pseudomonas Aeruginosa*. *Appl Environ Microbiol* **2012**, *78*, 5016–5020, doi:10.1128/AEM.00026-12. 367
368
369
31. Zhu, K.; Chen, S.; Sysoeva, T.A.; You, L. Universal Antibiotic Tolerance Arising from Antibiotic-Triggered Accumulation of Pyocyanin in *Pseudomonas Aeruginosa*. *PLoS Biol* **2019**, *17*, e3000573, doi:10.1371/journal.pbio.3000573. 370
371
372
32. Peng, B.; Su, Y.-B.; Li, H.; Han, Y.; Guo, C.; Tian, Y.; Peng, X.-X. Exogenous Alanine and/or Glucose plus Kanamycin Kills Antibiotic-Resistant Bacteria. *Cell Metab* **2015**, *21*, 249–261, doi:10.1016/j.cmet.2015.01.008. 373
374
33. Bhargava, P.; Collins, J.J.J. Boosting Bacterial Metabolism to Combat Antibiotic Resistance. *Cell Metab* **2015**, *21*, 154–155, doi:10.1016/j.cmet.2015.01.012. 375
376
34. Lopatkin, A.J.; Stokes, J.M.; Zheng, E.J.; Yang, J.H.; Takahashi, M.K.; You, L.; Collins, J.J. Bacterial Metabolic State More Accurately Predicts Antibiotic Lethality than Growth Rate. *Nat Microbiol* **2019**, 1–9, doi:10.1038/s41564-019-0536-0. 377
378
379
35. O’Toole, G.A. Microtiter Dish Biofilm Formation Assay. *J Vis Exp* **2011**, doi:10.3791/2437. 380
36. Ortori, C. a; Dubern, J.-F.; Chhabra, S.R.; Cámara, M.; Hardie, K.; Williams, P.; Barrett, D. a Simultaneous Quantitative Profiling of N-Acyl-L-Homoserine Lactone and 2-Alkyl-4(1H)-Quinolone Families of Quorum-Sensing Signaling Molecules Using LC-MS/MS. *Anal Bioanal Chem* **2011**, *399*, 839–850, doi:10.1007/s00216-010-4341-0. 381
382
383
384
37. Behrends, V.; Tredwell, G.D.; Bundy, J.G. A Software Complement to AMDIS for Processing GC-MS Metabolomic Data. *Anal Biochem* **2011**, *415*, 206–208. 385
386
38. Klausen, M.; Aaes-Jørgensen, A.; Molin, S.; Tolker-Nielsen, T. Involvement of Bacterial Migration in the Development of Complex Multicellular Structures in *Pseudomonas Aeruginosa* Biofilms. *Mol Microbiol* **2003**, *50*, 61–68, doi:10.1046/J.1365-2958.2003.03677.X. 387
388
389

39. Taylor, P.K.; Zhang, L.; Mah, T.-F. Loss of the Two-Component System TctD-TctE in *Pseudomonas Aeruginosa* Affects Biofilm Formation and Aminoglycoside Susceptibility in Response to Citric Acid. **2019**, doi:10.1128/mSphere.00102-19. 390
391
40. Liu, C.; Yang, J.; Liu, L.; Li, B.; Yuan, H.; Liu, W. Sodium Lactate Negatively Regulates *Shewanella Putrefaciens* CN32 Biofilm Formation via a Three-Component Regulatory System (LrbS-LrbA-LrbR). *Appl Environ Microbiol* **2017**, *83*, doi:10.1128/AEM.00712-17. 393
394
395
41. Novović, K.; Malešević, M.; Dinić, M.; Gardijan, L.; Kojić, M.; Jovčić, B. RclS Sensor Kinase Modulates Virulence of *Pseudomonas Capeferrum*. *Int J Mol Sci* **2022**, *23*, doi:10.3390/IJMS23158232/S1. 396
397
42. Kulasekara, H.D.; Ventre, I.; Kulasekara, B.R.; Lazdunski, A.; Filloux, A.; Lory, S. A Novel Two-Component System Controls the Expression of *Pseudomonas Aeruginosa* Fimbrial Cup Genes. *Mol Microbiol* **2005**, *55*, 368–380, doi:10.1111/J.1365-2958.2004.04402.X. 398
399
400
43. Anderson, G.G.; Moreau-Marquis, S.; Stanton, B.A.; O’Toole, G.A. In Vitro Analysis of Tobramycin-Treated *Pseudomonas Aeruginosa* Biofilms on Cystic Fibrosis-Derived Airway Epithelial Cells. *Infect Immun* **2008**, *76*, 1423–1433, doi:10.1128/IAI.01373-07. 401
402
403
44. Schobert, M.; Jahn, D. Anaerobic Physiology of *Pseudomonas Aeruginosa* in the Cystic Fibrosis Lung. *Int J Med Microbiol* **2010**, *300*, 549–556, doi:10.1016/j.ijmm.2010.08.007. 404
405
45. Sabra, W.; Lünsdorf, H.; Zeng, A.-P. Alterations in the Formation of Lipopolysaccharide and Membrane Vesicles on the Surface of *Pseudomonas Aeruginosa* PAO1 under Oxygen Stress Conditions. *Microbiology (Reading)* **2003**, *149*, 2789–2795, doi:10.1099/mic.0.26443-0. 406
407
408
46. Toyofuku, M.; Nomura, N.; Fujii, T.; Takaya, N.; Maseda, H.; Sawada, I.; Nakajima, T.; Uchiyama, H. Quorum Sensing Regulates Denitrification in *Pseudomonas Aeruginosa* PAO1. *J Bacteriol* **2007**, *189*, 4969–4972, doi:10.1128/JB.00289-07. 409
410
411
47. Gödeke, J.; Pustelny, C.; Häussler, S. Recycling of Peptidyl-TRNAs by Peptidyl-TRNA Hydrolase Counteracts Azithromycin-Mediated Effects on *Pseudomonas Aeruginosa*. *Antimicrob Agents Chemother* **2013**, *57*, 1617, doi:10.1128/AAC.02582-12. 412
413
414
48. Kolodkin-Gal, I.; Romero, D.; Cao, S.; Clardy, J.; Kolter, R.; Losick, R. D-Amino Acids Trigger Biofilm Disassembly. *Science* **2010**, *328*, 627–629, doi:10.1126/science.1188628. 415
416
49. Kao, W.T.K.; Frye, M.; Gagnon, P.; Vogel, J.P.; Chole, R. D-amino Acids Do Not Inhibit *Pseudomonas Aeruginosa* Biofilm Formation. *Laryngoscope Investig Otolaryngol* **2017**, *2*, 4, doi:10.1002/LIO.234. 417
418
50. Bredenbruch, F.; Geffers, R.; Nimtz, M.; Buer, J.; Häussler, S. The *Pseudomonas Aeruginosa* Quinolone Signal (PQS) Has an Iron-Chelating Activity. *Environ Microbiol* **2006**, *8*, 1318–1329, doi:10.1111/j.1462-2920.2006.01025.x. 419
420
421
51. Tettmann, B.; Niewerth, C.; Kirschhöfer, F.; Neidig, A.; Dötsch, A.; Brenner-Weiss, G.; Fetzner, S.; Overhage, J. Enzyme-Mediated Quenching of the *Pseudomonas* Quinolone Signal (PQS) Promotes Biofilm Formation of *Pseudomonas Aeruginosa* by Increasing Iron Availability. *Front Microbiol* **2016**, *7*, doi:10.3389/FMICB.2016.01978/FULL. 422
423
424
425
52. Kragh, K.N.; Hutchison, J.B.; Melaugh, G.; Rodesney, C.; Roberts, A.E.L.; Irie, Y.; Jensen, P.; Diggle, S.P.; Allen, R.J.; Gordon, V.; et al. Role of Multicellular Aggregates in Biofilm Formation. *mBio* **2016**, *7*, doi:10.1128/MBIO.00237-16. 426
427
428
53. Siryaporn, A.; Kuchma, S.L.; O’Toole, G.A.; Gitai, Z. Surface Attachment Induces *Pseudomonas Aeruginosa* Virulence. *Proc Natl Acad Sci U S A* **2014**, *111*, 16860–16865, doi:10.1073/pnas.1415712111. 429
430

54. Perinbam, K.; Chacko, J. v.; Kannan, A.; Digman, M.A.; Siryaporn, A. A Shift in Central Metabolism Accompanies Virulence Activation in *Pseudomonas Aeruginosa*. *mBio* **2020**, *11*, doi:10.1128/mBio.02730-18. 431-432
55. Chuang, S.K.; Vrla, G.D.; Fröhlich, K.S.; Gitai, Z. Surface Association Sensitizes *Pseudomonas Aeruginosa* to Quorum Sensing. *Nat Commun* **2019**, *10*, 4118, doi:10.1038/s41467-019-12153-1. 433-434
56. Vrla, G.D.; Esposito, M.; Zhang, C.; Kang, Y.; Seyedsayamdost, M.R.; Gitai, Z. Cytotoxic Alkyl-Quinolones Mediate Surface-Induced Virulence in *Pseudomonas Aeruginosa*. *PLoS Pathog* **2020**, *16*, e1008867, doi:10.1371/journal.ppat.1008867. 435-437
57. Laventie, B.-J.J.; Sangermani, M.; Estermann, F.; Manfredi, P.; Planes, R.; Hug, I.; Jaeger, T.; Meunier, E.; Broz, P.; Jenal, U. A Surface-Induced Asymmetric Program Promotes Tissue Colonization by *Pseudomonas Aeruginosa*. *Cell Host Microbe* **2019**, *25*, 140–152, doi:10.1016/j.chom.2018.11.008. 438-440
58. Nguyen, Y.; Sugiman-Marangos, S.; Harvey, H.; Bell, S.D.; Charlton, C.L.; Junop, M.S.; Burrows, L.L. *Pseudomonas Aeruginosa* Minor Pilins Prime Type IVa Pilus Assembly and Promote Surface Display of the PilY1 Adhesin. *J Biol Chem* **2015**, *290*, 601–611, doi:10.1074/jbc.M114.616904. 441-443
59. Persat, A.; Inclan, Y.F.; Engel, J.N.; Stone, H.A.; Gitai, Z. Type IV Pili Mechanistically Regulate Virulence Factors in *Pseudomonas Aeruginosa*. *Proc Natl Acad Sci U S A* **2015**, *112*, 7563–7568, doi:10.1073/pnas.1502025112. 444-446
60. Valentini, M.; Gonzalez, D.; Mavridou, D.A.; Filloux, A. Lifestyle Transitions and Adaptive Pathogenesis of *Pseudomonas Aeruginosa*. *Curr Opin Microbiol* **2018**, *41*, 15–20, doi:10.1016/J.MIB.2017.11.006. 447-448
61. Häussler, S.; Becker, T. The *Pseudomonas* Quinolone Signal (PQS) Balances Life and Death in *Pseudomonas Aeruginosa* Populations. *PLoS Pathog* **2008**, *4*, e1000166, doi:10.1371/journal.ppat.1000166. 449-450
62. Abdalla, M.Y.; Hoke, T.; Seravalli, J.; Switzer, B.L.; Bavitz, M.; Fliege, J.D.; Murphy, P.J.; Britigan, B.E. *Pseudomonas* Quinolone Signal Induces Oxidative Stress and Inhibits Heme Oxygenase-1 Expression in Lung Epithelial Cells. *Infect Immun* **2017**, *85*, doi:10.1128/IAI.00176-17. 451-453
63. Pezzoni, M.; Meichtry, M.; Pizarro, R.A.; Costa, C.S. Role of the *Pseudomonas* Quinolone Signal (PQS) in Sensitising *Pseudomonas Aeruginosa* to UVA Radiation. *J Photochem Photobiol B* **2015**, *142*, 129–140, doi:10.1016/J.JPHOTOBIOL.2014.11.014. 454-456
64. Bru, J.-L.; Rawson, B.; Trinh, C.; Whiteson, K.; Høyland-Kroghsbo, N.M.; Siryaporn, A. PQS Produced by the *Pseudomonas Aeruginosa* Stress Response Repels Swarms Away from Bacteriophage and Antibiotics. *J Bacteriol* **2019**, *201*, doi:10.1128/JB.00383-19. 457-459
65. Wright, G.D.; Hung, D.T.; Helmann, J.D. How Antibiotics Kill Bacteria: New Models Needed? *Nat Med* **2013**, *19*, 544–545, doi:10.1038/nm.3198. 460-462